UDC 541.6:547.12

A THEORETICAL STUDY OF THE SOLVENT EFFECT ON THE INTERACTION OF C_{20} AND N_2H_2

H. Alavi[1], R. Ghiasi[2]

[1]*Department of Chemistry, Kerman Branch, Islamic Azad University, Kerman, Iran*
[2]*Department of Chemistry, East Tehran Branch, Tehran, Islamic Azad University, Qiam Dasht, Iran*
 E-mail: rezaghiasi1353@yahoo.com, rghiasi@iauet.ac.ir

In this work, the interaction of C_{20} and the N_2H_2 fragment is investigated at the M062X/6-311G(d,p) level of theory in both gas and solution phases. The interaction energies obtained by the standard method are corrected by the basis set superposition error (BSSE) during the geometry optimization for all molecules at the same levels of theory. The results obtained from these calculations reveal that the interaction between C_{20} and N_2H_2 increases in the presence of more polar solvents. Values of the electrophilic charge transfer show the charge flow from C_{20} to N_2H_2. The influence of the solvent on the hyperpolarizability indicates that β_{tot} values decrease on passing from vacuum to the solution phase.

INTRODUCTION

The structure and properties of a C_{20} molecule have been investigated theoretically and experimentally [1—6]. This molecule is potentially the smallest fullerene. The synthesis and characterization of this molecule has been reported in the gas phase [7]. The remarkable structure of C_{20} has been the question of numerous theoretical researches [8, 9]. Fullerenes are considered as promising candidates for basic elements in nanoscale devices, and several instances of fullerene-based devices have been already considered both experimentally and theoretically [10, 11]. The modification of C_{20} is a matter of common attention for experimentalists and theoreticians to get insight into the structural as well as electronic properties. The structure and properties of fullerene C_{20} and its derivatives $C_{20}(C_2H_2)_n$ and $C_{20}(C_2H_4)_n$ ($n = 1$—4) have been explored [12], and they illustrate that the most stable fullerene C_{20} and its derivatives $C_{20}(C_2H_2)_n$ and $C_{20}(C_2H_4)_n$ ($n = 1$—3) exhibit significant aromaticity, while $C_{20}(C_2H_2)_4$ and $C_{20}(C_2H_4)_4$ have no spherical aromaticity. Furthermore, heteroatom impacts on the structure, stability, and aromaticity of X_nC_{20-n} fullerenes have been established [13]. The interaction of C_{20} with N_2X_2 (X = H, F, Cl, Br, Me) has been investigated theoretically [14]. The structure, aromaticity, frontier orbital analysis, and the natural bond analysis of $C_{20}…N_2X_2$ molecules have been explored, and the influence of the basis set and methods on the structure and interaction energies of these molecules have been investigated.

N_2H_2 (diazene) was suggested as early as 1892 to be a reactive intermediate in the decomposition of azoformic acid [15]. Nonetheless, it was not detected before 1958 when Foner and Hudson identified N_2H_2 by mass spectroscopy while investigating hydrazoic acid in an electrical discharge [16].

Due to biological and industrial importance of reduced nitrogen species, many chemists have tried to prepare analogous model complexes, which has led to the generation of a large number of transition metal dinitrogen, diazene, and hydrazine complexes [17—19].

It is well known that a solvent plays an important role in physical and chemical processes. The presence of specific and non-specific interactions between the solvent and the solute molecules is responsible for the change in several properties such as the molecular geometry, the electronic structure, and the dipole moment of the solute. In the present work, extensive theoretical calculations of fullerene C_{20} and their interactions with N_2H_2 have been performed in both gas and solution phases. The structure, frontier orbital analysis, and hyperpolarizability of $C_{20}...N_2H_2$ have been explored. Furthermore, the influence of the solvent on the structural properties of the $C_{20}...N_2H_2$ molecule is discussed. We expect that the guidelines established for this $C_{20}...N_2H_2$ system in solution can be extended to all the above-mentioned molecules belonging to the same class and that a structure stability correlation can be established.

COMPUTATIONAL METHODS

All calculations were carried out with the Gaussian 09 suite program [20]. The calculations of systems containing C, H and N are described by the standard 6-311G(d,p) basis set [21—24]. The geometry optimization was performed with the hybrid functional of Truhlar and Zhao (M062X) [25].

A vibrational analysis was performed at each stationary point found, which confirms its identity as an energy minimum.

The interaction energy, IE, can be evaluated from the difference between the energy of the molecule and sum of the energies of C_{20} and N_2H_2

$$I.E = E(C_{20}...N_2H_2) - [E(C_{20}) + E(N_2H_2)].$$

The calculated interaction energies were corrected for basis set superposition errors (BSSE), which were computed in all calculations using the counterpoise correction method of Boys and Bernardi [26]. This error is due to the different number of basis functions included in the molecule and monomer calculations. Since the molecule employs a basis set larger than the one employed by monomers, in most cases, this error models the molecule to be too attractive. As it has been studied before, when BSSE is corrected along the whole surface, important changes in the potential energy surface appear, not only in the energy but also in the position of the minimum as well as its topology [27, 28].

Geometries were optimized at this level of theory without any symmetry constraints followed by the calculations of the first order hyperpolarizabilities. The total static first hyperpolarizability β was obtained from the following equations:

$$\beta_{tot} = \sqrt{\beta_x^2 + \beta_y^2 + \beta_z^2}$$

upon calculating the individual static components

$$\beta_i = \beta_{iii} + \frac{1}{3}\sum_{i \neq j}(\beta_{ijj} + \beta_{jij} + \beta_{jji}).$$

Due to the Kleinman symmetry [29]

$$\beta_{xyy} = \beta_{yxy} = \beta_{yyx}; \quad \beta_{yyz} = \beta_{yzy} = \beta_{zyy}, \ldots$$

one finally obtains the equation that has been employed

$$\beta_{tot} = \sqrt{(\beta_{xxx} + \beta_{xyy} + \beta_{xzz})^2 + (\beta_{yyy} + \beta_{yzz} + \beta_{yxx})^2 + (\beta_{zzz} + \beta_{zxx} + \beta_{zyy})^2}.$$

We have studied the solvation effects using the self-consistent reaction field (SCRF) approach, in particular, using the polarizable continuum model (PCM) [30]. Using this method, the geometry of the studied molecule was re-optimized and the hyperpolarizability was calculated by the same functionals and basis sets.

The GaussSum 2.2 software package was used to evaluate the detailed analysis of the atomic orbital contributions to the complex [31].
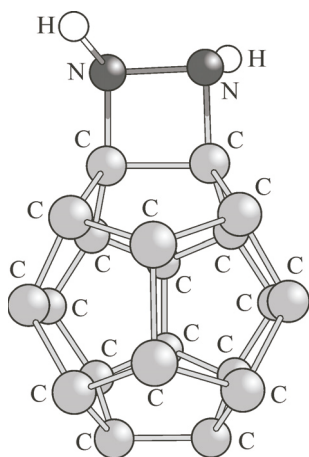
Fig. 1. Structure of the $C_{20}...N_2H_2$ molecule

RESULTS AND DISCUSSION

Interaction energies and dipole moments. The computed interaction energies (I.E) for the $C_{20}...N_2H_2$ molecule (Fig. 1) in the gas phase and various solvents have been gathered in Table 1. It can be expected that the interaction between C_{20} and N_2H_2 increases in the presence of more polar solvents. Fig. 2, *a* presents a good correlation between the interaction energies and dielectric constants of solvents. On the other hand, the comparison of the interaction energy value in the gas phase and the solution phase show a geater interaction between C_{20} and N_2H_2 in the solution phase.

The interaction energy in the gas phase was corrected for BSSE. The uncorrected interaction energy is –57.88 kcal/mol and BSSE amounts to less than 8.05 % of the raw interaction energy.

On the other hand, the energies of stabilization by solvents (solvation energy, E_{solv}) have been calculated (Table 1). These values are the relative energy of the title compound in a solvent and that in the gas phase. As we can see the solvation energies are dependent on the dielectric constant of solvents, and these values decrease with an increase in the dielectric constants of solvents. As a result, the stability of the $C_{20}...N_2H_2$ molecule increases in more polar solvents. This is because a dipole in the molecule induces a dipole in the medium, and the electric field applied to the solute by the solvent (reaction) dipole in turn interacts with the molecular dipole to result in net stabilization. Hence, the $C_{20}...N_2H_2$ molecule is more stable in polar solvent rather than in the gas phase. There is a good correlation between dielectric constants and E_{solv}

$$E_{solv} = -0.100\varepsilon - 1.957; \quad R^2 = 0.941.$$

T a b l e   1

Absolute energy (Hartree), *interaction energies* (kcal/mol), *solvation energy* (E_{solv}, kcal/mol), N—N, C—N *bond distances* (*in* Å) *for the* $N_2H_2...C_{20}$ *molecule in the gas phase and different solvents*

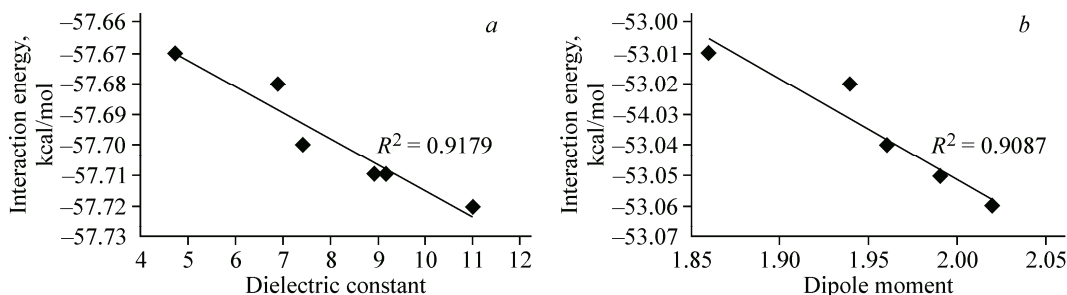| Phase	ε	I.E	E_{solv}	R(N—N, in molecule)	R(NN, N_2H_2)	R(C...N)
Gas	—	–57.88	—	1.48202	1.23320	1.4718
Chloroform	4.71	–57.67	–2.359	1.48354	1.23341	1.4720
Aniline	6.89	–57.68	–2.698	1.48364	1.23345	1.4720
THF	7.42	–57.70	–2.754	1.48365	1.23332	1.4719
Dichloromethane	8.93	–57.71	–2.879	1.48365	1.23334	1.4720
Quinoline	9.16	–57.71	–2.894	1.48369	1.23334	1.4720
Isoquinoline	11.00	–57.72	–2.999	1.48372	1.23335	1.4720

Fig. 2. Dependence of the interaction energy and (*a*) dielectric constant and (*b*) dipole moment in the $C_{20}...N_2H_2$ molecule

Dipole moment (Debye) *and isotropic and anisotropic polarizability values* (*in* Bohr^3) *for the* $N_2H_2…C_{20}$ *molecule in the gas phase and different solvents*

Phase	μ	α_{xx}	α_{yy}	α_{zz}	α_{iso}	α_{aniso}
Gas	1.36	205.772	171.869	168.669	182.1033	35.611
Chloroform	1.86	281.52	239.15	234.89	251.85	44.65
Aniline	1.94	293.96	251.19	246.68	263.94	45.20
THF	1.96	296.08	253.26	248.71	266.02	45.27
Dichloromethane	1.99	300.84	257.95	253.29	270.69	45.40
Quinoline	1.99	301.45	258.55	253.88	271.29	45.41
Isoquinoline	2.02	305.48	262.57	257.81	275.29	45.49

The dipole moments of the $C_{20}…N_2H_2$ molecule in the gas phase and different solvents have been listed in Table 2. As seen in Table 2, the $C_{20}…N_2H_2$ molecule has a less dipole moment in the gas phase. In the solution phase, dipole moments increase with increasing polarity of the solvents. Also, these values show a good relationship with the interaction energies (Fig. 2, *b*).

Polarizability. Values of the isotropic and anisotropic polarizability for the $C_{20}…N_2H_2$ molecule in the gas phase and different media obtained using the PCM model are listed in Table 2. The polarizability is the measure of a molecule distortion in an electric field.

As seen in Table 2, the $C_{20}…N_2H_2$ molecule has less polarizability in the gas phase. These values show that the solvent effect on the isotropic and anisotropic polarizabilities is in parallel with that on the dipole moment of the solute. There is a good linear relationship between the isotropic and anisotropic polarizabilities with the dipole moments of the $C_{20}…N_2H_2$ molecule in the set of solvents ($R^2 = 0.998$, and 0.971, respectively). Namely, there is the larger dipole moment of the solute and the higher isotropic polarizability in more polar solvents. Also, there is a good correlation between the Isotropic polarizability and the dielectric constant where the correlation coefficient is 0.948.

Thermochemical analysis. Thermochemical analysis is studied for all molecules. The ΔH, ΔG, and K values are reported in Table 3 in which the individual terms are referred to a temperature of 298 K. The reaction can be considered as

$$C_{20} + N_2H_2 \rightarrow C_{20}…N_2H_2.$$
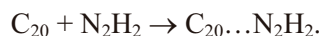
As can be verified, the ΔG values increase in the solution phase. The equilibrium constants of all molecules are given in Table 3. This shows that the equilibrium constant is highest in the vacuum phase.

Bond distances. The NN and C…N bond distances of the $C_{20}…N_2H_2$ molecule in the gas phase and different solvents have been collected in Table 1. As seen in Table 1, the CC, NN, and CN bond lengths increase in the solution phase. There is a minor dependence between the bond distances and the dielectric constants. The comparison of NN bond distances of free N_2H_2 and the $C_{20}…N_2H_2$ molecule show an increase in this bond in the $C_{20}…N_2H_2$ molecule. This increase in the bond length (ΔR) has good correlation with the dielectric constant of the solvents

$$\Delta R = -0.004\varepsilon - 0.028; \quad R^2 = 0.935.$$

Thermochemical parameters for the $N_2H_2…C_{20}$ *molecule in the gas phase and different solvents*

Phase	ΔG, kcal/mol	ΔH, kcal/mol	K	Phase	ΔG, kcal/mol	ΔH, kcal/mol	K
Gas	−40.477	−53.831	4.84E+29	Dichloromethane	−39.448	−53.695	8.52E+28
Chloroform	−39.872	−53.698	1.74E+29	Quinoline	−39.448	−53.695	8.53E+28
Aniline	−39.876	−53.709	1.75E+29	Isoquinoline	−39.453	−53.702	8.60E+28
THF	−39.443	−53.688	8.46E+28				

Frontier orbital energies (*in* a.u.), HOMO—LUMO *gap* (*in* eV), *hardness* (*in* eV), *chemical potential* (*in* eV), *electrophilicity* (*in* eV) *and* ECT *for the* $N_2H_2...C_{20}$ *molecule in the gas phase and different solvents*

Phase	E(HOMO)	E(LUMO)	ΔE	η	μ	ω	ECT
Gas	−0.2624	−0.0994	4.436	2.218	−4.922	5.461	1.453
Chloroform	−0.2611	−0.0975	4.453	2.226	−4.878	5.345	1.406
Aniline	−0.2610	−0.0972	4.457	2.228	−4.874	5.330	1.401
THF	−0.2610	−0.0972	4.458	2.229	−4.873	5.328	1.400
Dichloromethane	−0.2610	−0.0971	4.459	2.230	−4.872	5.322	1.399
Quinoline	−0.2610	−0.0971	4.459	2.230	−4.871	5.321	1.398
Isoquinoline	−0.2609	−0.0970	4.461	2.230	−4.870	5.317	1.397

Molecular orbital analysis. The energies of the frontier orbitals (HOMO, LUMO) along with the corresponding HOMO—LUMO energy gaps for the $C_{20}...N_2H_2$ molecule in the gas phase and different solvents are given in Table 4.

The frontier orbital distribution in the $C_{20}...N_2H_2$ molecule is plotted in Fig. 3. Fig. 3 shows that the HOMO and LUMO are distributed mainly on C_{20}. The contribution of the N_2H_2 fragment to the HOMO is minor, but there is no contribution to LUMO. Energies and the percentage composition in terms of the defined groups of the frontier orbitals show that the largest contributions to the HOMO arise from the cage (96.0 %). On the other hand, the largest contributions to the LUMO arise from the cage (100 %).

The inclusion of solvation effects leads also to changes in the molecular orbital energies (Table 4). In solution, the HOMO and LUMO are destabilized, with respect to the corresponding values in vacuum.

Also, the HOMO—LUMO gap and the hardness of the $C_{20}...N_2H_2$ molecule in the solution phase are more than those in the gas phase. A good relationship exists between the HOMO—LUMO gap and the polarity of solvents ($R^2 = 0.954$). The variations in this property may be illustrated by considering the fact that neutral or charged species enhance their effective radii in the solution phase. This signifies that the electrostatic potential q/r will forever diminish from the gas phase to the solution phase. As a result, solvated species reduce their effective hardness and subsequently, become softer in the solution phase [32].

Chemical reactivity. *Global reactivity descriptors.* Global reactivity descriptors [33—36], the chemical potential (μ), the global hardness (η), the electrophilicity index (ω), and the electrophilic charge transfer (ECT) determined based on the Koopman′s theorem[37] for the reactant $C_{20}...N_2H_2$ system are listed in Table 4.
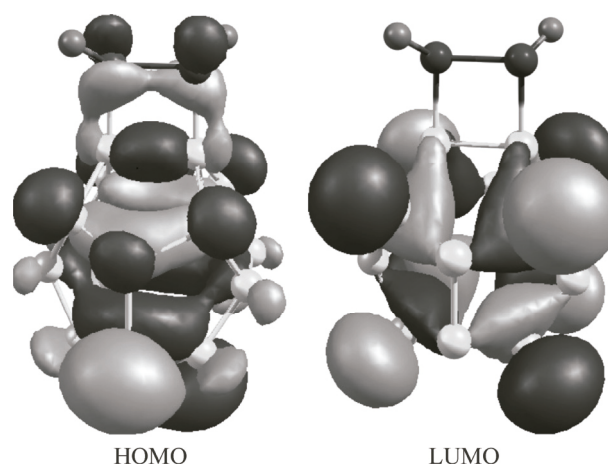

HOMO   LUMO

Fig. 3. Frontier orbital distributions in the $C_{20}...N_2H_2$ system

$$\mu = \frac{E(\mathrm{HOMO}) + E(\mathrm{LUMO})}{2},$$

$$\eta = \frac{E(\mathrm{LUMO}) + E(\mathrm{HOMO})}{2}.$$

where I and A are the ionization potential and the electron affinity, respectively and $I = -E(\mathrm{HOMO})$ and $A = -E(\mathrm{LUMO})$. The chemical potential of DFT measures the escaping tendency of electrons from the system. The response of the chemical potential to changes in the number of electrons is called the chemical hardness.

When the interaction between C_{20} and N_2H_2 increases, the highest hardness values are observed. Thus, there is a good linear correlation between the interaction energies and the hardness values ($R^2 = 0.949$).

ECT of the $C_{20}\ldots N_2H_2$ molecule in gas and various solvents has been reported in Table 4. ECT is defined as the difference between ΔN_{max} values of interacting molecules

$$\mathrm{ECT} = \Delta N_{max}(N_2H_2) - \Delta N_{max}(C_{20}).$$

In this equation ΔN_{max} is defined as

$$(\Delta N_{max \square})_i = \frac{\mu_i}{\eta_i}.$$

The positive values of ECT reveal the charge flow from C_{20} to N_2H_2. On the other hand, these values show a decrease in charge transfer with increasing solvent polarity.

Hyperpolarizability. It is illustrated that the solvent polarity plays an important role in the first hyperpolarizabilities in dipolar molecules. The β_{tot}, β_x, β_y, β_z values of the $C_{20}\ldots N_2H_2$ molecule in different solvents have been calculated. These values indicate that β_{tot} values decrease from vacuum to the solution phase ($\beta_{total} = 0.0$ for C_{20}). The dependence of the first hyperpolarizability of the studied compound on both dielectric constant of the media and Onsager function has been investigated [38]. Fig. 4 is typical of a dipolar reaction field interaction in the solvation process [38—41]. Therefore, the electronic reorganization in solution for the $C_{20}\ldots N_2H_2$ molecule makes an important effect on the resulting first hyperpolarizabilities.

CONCLUSIONS

In this study, we showed that the interaction energy values increase from vacuum to different solvents and the interaction between C_{20} and N_2H_2 increases with increasing dielectric constant of solvents. Based on the interaction energy values, the synthesis of the $C_{20}\ldots N_2H_2$ system is possible and the most interaction occurs in more polar solvents. In solution, HOMO and LUMO energies, hardness and chemical potential values increased with respect to the corresponding values in vacuum. On the other hand, electrophilicty values decreased in the solution phase. The β_{tot} values increase from vacuum to different solvents and rise in more polarity. The positive ECT values reveal the charge flow from C_{20} to N_2H_2 and the charge transfer decreases with increasing solvent polarity.
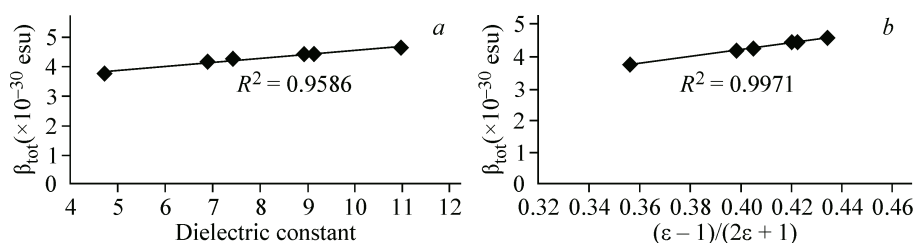

Fig. 4. Dependence of the hyperpolarizability on the dielectric constant (*a*) and the Onsager function (*b*) for the $C_{20}\ldots N_2H_2$ molecule

REFERENCES

1. *Grossman J.C., Mitas L., Raghavachari K.* // Phys. Rev. Lett. – 1995. – **750**. – P. 3870 – 3873.
2. *Bylaska E.J., Taylor P.R., Kawai R., Weare J.H.* // J. Phys. Chem. A. – 1996. – **100**. – P. 6966 – 6972.
3. *Taylor R., Bylaska E., Weare J.H., Kawai R.* // Chem. Phys. Lett. – 1995. – **235**. – P. 558 – 563.
4. *Wang Z., Day P., Pachte R.* // Chem. Phys. Lett. – 1996. – **248**. – P. 121 – 126.
5. *Jan M.L.M., El-Yazal J.* // Chem. Phys. Lett. – 1996. – **248**. – P. 345 – 352.
6. *Sokolova S., Luchow A., Anderson J.B.* // Chem. Phys. Lett. – 2000. – **323**. – P. 229 – 233.
7. *Prinzbach H., Weiler A., Landenberger P., Wahl F., Worth J., Scott L.T., Gelmont M.D., Olevano D., Issen-dorff B.V.* // Nature. – 2000. – **60**. – P. 407.
8. *Luo J., Peng L.M., Xue Z.Q., Wu J.L.* // J. Chem. Phys. – 2004. – **120**. – P. 7998 – 8001.
9. *Chen Z., Heine T., Jiao H., Hirsch A., Thiel W., Schleyer P.v.R.* // Chem. Eur. J. – 2004. – **10**. – P. 963 – 970.
10. *Taylor J., Guo H., Wang J.* // Phys. Rev. B. – 2001. – **63**. – P. 121104 – 121108.
11. *Zeng D., Wang H., Wang B., Hou J.G.* // Appl. Phys. Lett. – 2000. – **77**. – P. 3595 – 3597.
12. *Zhanga C., Sun W., Caob Z.* // J. Chem. Phys. – 2007. – **126**. – P. 144306.
13. *Kassaee M.Z., Buazar F., Koohi M.* // J. Mol. Structure: THEOCHEM. – 2010. – **940**. – P. 19 – 28.
14. *Ghiasi R., Fashami M.Z.* // J. Theor. Comput. Chem. – 2014. – **13**. – P. 1450041.
15. *Qhiele J., Liebigs J.* // Ann. Chem. – 1892. – **271**. – P. 127.
16. *Foner S.N., Hudson R.L.* // J. Chem. Phys. – 1958. – **28**. – P. 719 – 719.
17. *Paulat F., Lehnert N., Ishikawa Y., Okamoto K.-I., Fujisawa K.* // Inorg. Chim. Acta. – 2008. – **361**. – P. 901 – 915.
18. *Sellmann D., Sutter J.* // Acc. Chem. Res. – 1997. – **30**. – P. 460 – 469.
19. *Sellmann D., Hille A., Rosler A., Heinemann F.W., Moll M., Brehm G., Schneider S., Reiher M., Hess B.A., Bauer W.* // Chem. Eur. J. – 2004. – **10**. – P. 819.
20. *Frisch M.J., Trucks G.W., Schlegel H.B., Scuseria G.E., Robb M.A., Cheeseman J.R., Scalman G., Barone V., Mennucci B., Petersson G.A., Nakatsuji H., Caricato M., Li X., Hratchian H.P., Izmaylov A.F., Bloino J., Zheng G., Sonnenberg J.L., Hada M., Ehara M., Toyota K., Fukuda R., Hasegawa J., Ishida M., Nakajima T., Honda Y., Kitao O., Nakai H., Vreven T., Montgomery J.A. Jr., Peralta J.E., Ogliaro F., Bearpark M., Heyd J.J., Brothers E., Kudin K.N., Staroverov V.N., Kobayashi R., Normand J., Raghavachari K., Rendell A., Burant J.C., Iyengar S.S., Tomasi J., Cossi M., Rega N., Millam J.M., Klene M., Knox J.E., Cross J.B., Bakken V., Adamo C., Jaramillo J., Gomperts R., Stratmann R.E., Yazyev O., Austin A.J., Cammi R., Pomel-li C., Ochterski J.W., Martin R.L., Morokuma K., Zakrzewski V.G., Voth G.A., Salvador P., Dannenberg J.J., Dapprich S., Daniels A.D., Farkas O., Foresman J.B., Ortiz J.V., Cioslowski J., Fox D.J.* In, Gaussian, Inc., Wallingford CT, 2009.
21. *Krishnan R., Binkley J.S., Seeger R., Pople J.A.* // J. Chem. Phys. – 1980. – **72**. – P. 650 – 654.
22. *Wachters A.J.H.* // J. Chem. Phys. – 1970. – **52**. – P. 1033 – 1036.
23. *Hay P.J.* // J. Chem. Phys. – 1977. – **66**. – P. 4377 – 4384.
24. *McLean A.D., Chandler G.S.* // J. Chem. Phys. – 1980. – **72**. – P. 5639 – 5648.
25. *Zhao Y., Truhla D.G.* // J. Phys. Chem. – 2006. – **110**. – P. 5121 – 5129.
26. *Boys S.F., Bernardi F.* // Mol. Phys. – 1970. – **19**. – P. 553 – 556.
27. *Simon S., Duran M., Dannenberg J.J.* // J. Chem. Phys. – 1996. – **105**. – P. 11024.
28. *Salvador P., Simon S., Duran M., Dannenberg J.J.* // J. Chem. Phys. – 2000. – **13**. – P. 5666.
29. *Keleiman D.A.* // Phy. Rev. – 1962. – **126**. – P. 1977.
30. *Tomasi J., Mennucci B., Cammi R.* // Chem. Rev. – 2005. – **105**. – P. 2999 – 3093.
31. *O'Boyle N.M., Tenderholt A.L., Langner K.M.* // J. Comp. Chem. – 2008. – **29**. – P. 839 – 845.
32. *Pearson R.* // J. Am. Chem. Soc. – 1986. – **108**. – P. 6109.
33. *Pearson R.G.* // J. Org. Chem. – 1989. – **54**. – P. 1430 – 1432.
34. *Parr R.G., Pearson R.G.* // J. Am. Chem. Soc. – 1983. – **105**. – P. 7512 – 7516.
35. *Geerlings P., Proft F.D., Langenaeker W.* // Chem. Rev. – 2003. – **103**. – P. 1793 – 1874.
36. *Parr R.G., Szentpály L., Liu S.* // J. Am. Chem. Soc. – 1999. – **121**. – P. 1922 – 1924.
37. *Parr R.G., Yang W.* Density functional Theory of Atoms and Molecules. – Oxford University Press, Oxford, New York, 1989.
38. *Onsager L.* // J. Am. Chem. Soc. – 1936. – **58**. – P. 1486.
39. *Clays K., Persoons A.* // Phys. Rev. Lett. – 1991. – **66**. – P. 2980.
40. *Lee H., An S.-Y., Cho M.* // J. Phys. Chem. B. – 1999. – **103**. – P. 4992.
41. *Ray P.C., Leszczynski J.* // Chem. Phys. Lett. – 2004. – **399**. – P. 162.